A Self-Folding Polymer Film Based on Swelling Metal-Organic Frameworks

Javier Troyano,[a] Arnau Carné-Sánchez,[a] Javier Pérez-Carvajal,[a] Laura León-Reina,[b] Inhar Imaz,[a] Aurelio Cabeza,[c] Daniel Maspoch*[a,d]

[a] Catalan Institute of Nanoscience and Nanotechnology (ICN2), CSIC and BIST Campus UAB, Bellaterra, 08193 Barcelona, Spain [b] Servicios Centrales de Apoyo a la Investigación, Universidad de Málaga, 29071 Málaga, Spain
[c] Dpto Química Inorgánica, Cristalografía y Mineralogía, Campus de Teatinos s/n, Universidad de Málaga, 29071 Málaga, Spain
[d] ICREA Pg. Lluís Companys 23, Barcelona, 08010, Spain
E-mail: daniel.maspoch@icn2.cat

Abstract

Here, we exploit the well-known swelling behaviour of metal-organic frameworks (MOFs) to create a self-folding polymer film. Namely, we show that incorporating crystals of the flexible MOF MIL-88A into a polyvinylidene difluoride (PVDF) matrix affords a polymer composite film that undergoes reversible shape transformations upon exposure to polar solvents and vapours. Since the self-folding properties of this film correlate directly with the swelling properties of the MIL-88A crystals, it selectively bends to certain solvents and its degree of folding can be controlled by controlling the relative humidity. Moreover, it shows a shape-memory effect at relative humidity values from 60% to 90%. As proof-of-concept, we demonstrate that these composite films can lift cargo and can be used to assemble 3D structures from 2D patterns. Our strategy is a straightforward method for designing autonomous soft materials whose folding properties can be tuned by judicious choice of the constituent flexible MOF.

Keywords: metal-organic framework • swelling behaviour • self-folding • composite • film

Among the most fascinating properties of certain metal–organic frameworks (MOFs) is their structural flexibility in response to external stimuli. Contrary to rigid crystalline porous materials (*e.g.* zeolites or aluminophosphates), the highly ordered networks of flexible MOFs, also known as *soft porous crystals*,[1] can undergo reversible dynamic structural transformations.[2] This flexibility arises from the reversible nature of coordination bonds and weaker supramolecular interactions within MOFs, which allow for conformational changes of secondary building units and organic linkers. Over the past decade, this intriguing aspect of MOF chemistry has been investigated, leading to the discovery of numerous structural-transition phenomena, including thermal expansion,[3] linker rotation,[4] and subnetwork displacement.[5] Among the most interesting of flexible MOFs are swelling MOFs, which undergo expansion or contraction due to adsorption or desorption, respectively.[6] A prime example is the isoreticular Fe(III) dicarboxylate MIL-88 family (MIL: Materials from Institute Lavoisier), in which the MOF unit-cell volume exhibits reversible enlargement upon adsorption of polar solvent molecules, due to the formation of hydrogen bond interactions between guest molecules and the framework.[7] In these MOFs, the swelling can be strongly influenced by the solvent and by the functional groups in the linkers.[8] Beyond molecular-

level changes, a remarkable effect of such lattice swelling is the subsequent macroscopic deformation of the crystals.[8b]

Our group considered that the aforementioned phenomenon had been overlooked in the development of functional materials, so we began to reflect on how such swelling motion might be exploited to develop novel soft materials capable of reversible shape transformations. In this regard, *self-folding materials*, which are able to translate external stimuli such as thermal, light, electrical or chemical energy into useful and predictable shape transformations, are garnering attention for their potential utility in applications such as robotics,[9] artificial muscles,[10] energy harvesting,[11] and encapsulation.[12] Nature is the principal source of inspiration for development of these materials.[13] For instance, plant tissues have developed diverse mechanisms for reversible and efficient shape transformations, which are typically driven by ambient humidity variations.[14] The underlying principle behind self-folding materials is the differential swelling/shrinking throughout a non-homogenous structure. These anisotropic architectures can be easily generated by coupling two materials that have distinct mechanical properties, as in the case of (multi)bilayers,[15] or by designing more-complex monolayer materials in which vertical, lateral or programmed gradient patterns are created.[16] Over the past few years, researchers have developed numerous strategies for the fabrication of self-folding monolayer materials, including differential cross-linking;[17] varying degree of order[18] or hydrophobicity;[19] lithographic methods;[20] and crystal-phase anisotropy.[21] One attractive approach is the fabrication of composite materials in which guest and host components differ in their respective swelling capacity. This is typically done by embedding non-swellable (or less swellable) fillers into a swellable polymeric matrix.[22] Interestingly, researchers have recently created a self-folding composite film through the opposite strategy: they incorporated swellable cyclopentanone as guest into a non-swellable polymer host.[23]

Here, we report the development of a new type of self-folding composite films fabricated by integrating flexible MOF crystals as fillers into a passive polymer matrix. Note that this type of composite films are known as mixed matrix membranes in separation processes.[24] To synthesise these films, we chose MIL-88A as a representative swelling MOF, and polyvinylidene difluoride (PVDF) as the passive polymer matrix. The resulting film (hereafter called *MIL-88A@PVDF*) exhibited self-folding in response to solvents (*e.g.* water and methanol) that induce swelling in the MIL-88A crystals. We believe that our proof-of-concept film confirms that the swelling properties of flexible MOFs can be transferred from the molecular scale to a functional macroscopic object.

We began by synthesising MIL-88A microcrystals. To this end, a mixture of $FeCl_3 \cdot 6H_2O$ and fumaric acid solution in DMF was heated at 85 ºC overnight (Supporting Information, Figures S1-S4). Field-emission scanning electron microscopy (FESEM) revealed the formation of microcrystals ranging from 0.5 µm to 9.0 µm in size (Supporting Information, Figure S2). Next, a single crystal of this MIL-88A was subjected to progressively increasing levels of relative humidity and studied for morphological changes via humidity-controlled environmental FESEM analysis.[25] As shown in Figures 1a and S3, an increase in relative humidity from 20% to 90% led to a gradual decrease (overall: ~ 18%) in crystal length and a gradual increase (overall: ~ 33%) in crystal width, translating to an overall increase of ~ 45% in total crystal volume at 90% relative humidity. When the relative humidity was decreased back down to 20%, the crystal recovered its initial dimensions, thus exhibiting a reversible swelling/shrinkage process (Supporting Information, Figure S3). These results are in concordance with the previously described swelling behaviour of MIL-88A in water, whereby the *a* cell parameter gradually increases while the *c* parameter decreases.[7b]

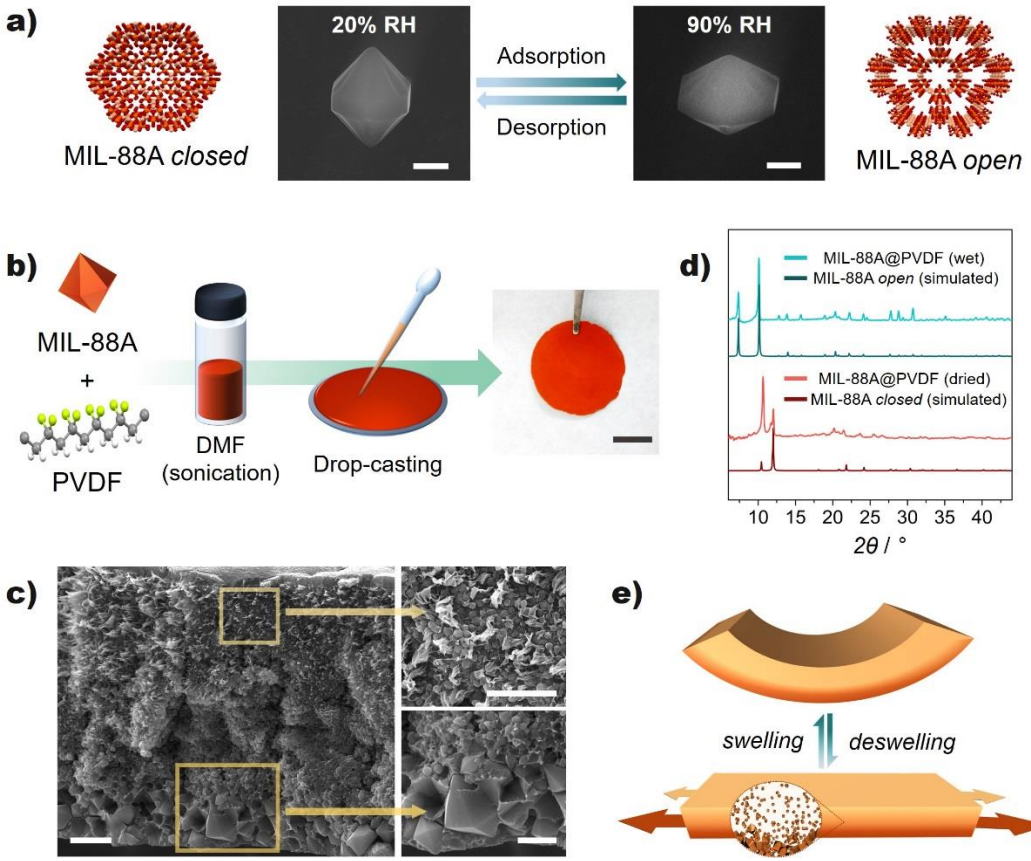

Figure 1 a) Schematic representation of the swelling behaviour of MIL-88A, together with the corresponding environmental FESEM images of an individual crystal of MIL-88A at relative humidity values of 20% (left) and 90% (right). Scale bar = 5 µm. b) Schematic representation of the synthetic procedure used to prepare the MIL-88A@PVDF films, and a photograph of a prepared film. Scale bar = 2 cm. c) Cross-sectional FESEM image of a MIL-88A@PVDF film, and magnified images (right) of its top (left, top) and bottom (left, bottom) sides. Scale bars = 10 µm (left) and 5 µm (right). d) XRPD images of a MIL-88A@PVDF film after activation at 120 ºC (red) or immersion in water (blue), compared with the respective simulated closed and open structures of MIL-88A. e) Schematic representation of the folding mechanism of the MIL-88A@PVDF films.

We then fabricated MIL-88A@PVDF films by drop-casting a homogeneous suspension of MIL-88A crystals in a DMF solution of the PVDF polymer, onto a silicon wafer.[26] The spread suspension was then dried at 140 ºC for 30 min in a pre-heated oven to afford the films (Figure 1b). The optimum MOF loading in these films was 50 wt%, as a higher MOF content resulted in brittle, cracked films and a lower MOF loading (*e.g.* 10 and 30 wt%) resulted in a depletion of the folding response (Supporting Information, Figure S5). Note also that for formation of dense MIL-88A@PVDF films[27] -a condition that is necessary for the efficient propagation of the strain caused by swelling/shrinkage motion of the individual crystals embedded in the polymeric matrix- the optimal temperature was found to be 140 ºC. Here, cross-sectional FESEM images of the films confirmed the formation of a dense, polymeric PVDF network (thickness: ~ 70 □m), in which the smaller MIL-88A crystals are homogeneously embedded throughout the film, and the larger crystals accumulate at the bottom side (*i.e.* the side that had been in contact with the silicon wafer during film fabrication; Figures 1c and S6). This heterogeneous distribution of MIL-88A crystals throughout the MIL-88A@PVDF films creates the kind of anisotropy that is required for self-folding.

We first studied the folding capacity of the fabricated films by immersing MIL-88A@PVDF strips with the maximum MOF content (50 wt%) in various solvents, including water, methanol, ethanol, *tert*-butanol, acetonitrile, acetone, chloroform, toluene, and *n*-pentane.

Uniform strips (3 cm x 1 cm) of a MIL-88A@PVDF film were obtained by cutting it with scissors. In this systematic study, the MIL-88A@PVDF strips immersed in water, methanol, ethanol, acetonitrile or acetone instantaneously folded, whereas those immersed in *tert*-butanol, chloroform, toluene or *n*-hexane remained unaltered (Supporting Information, Figure S7a). Moreover, upon drying at 120 ºC, the bended strips recovered their original (flat) shape. An initial interesting observation was that the solvents that induced reversible swelling in the MIL-88A crystals were the same ones that induced reversible folding in the strips. The correlation between film folding and swelling behaviour was further corroborated by X-ray powder diffraction (XRPD) (Figure 1d): prepared samples of flat strips and dried MIL-88A crystals both exhibited the XRPD pattern characteristic of the closed form of MIL-88A. However, after immersing these samples into water, methanol, ethanol, acetonitrile or acetone, their corresponding XRPD patterns revealed the characteristic transition from the closed form to the open form of MIL-88A. Contrariwise, the XRPD patterns of MIL-88A@PVDF strips or MIL-88A crystals immersed into the other solvents indicated that materials retained the closed form of MIL-88A (Supporting Information, Figure S7b). Interestingly, the MIL-88A@PVDF strips always bent from the bottom side upwards, as indicated in Figure 1e. We attributed this behaviour to the higher strain caused by the expansion/contraction of the larger MIL-88A crystals present mainly on the bottom side of the film.

To further correlate the folding behaviour of these MIL-88A@PVDF films with the structural flexibility of MIL-88A crystals, we compared the self-folding properties of MIL-88A@PVDF films to those of a bare PVDF film in the absence of MIL-88A crystals, and to those of PVDF films containing microscale crystals of the non-flexible MOFs MIL-100 and MOF-801 (these films are hereafter called *Fe-MIL-100@PVDF* and *MOF-801@PVDF*, respectively; Supporting Information, Figures S8-S17). To this end, the response of each film was evaluated upon immersion of the corresponding strips into the aforementioned solvents (Supporting Information, Figure S17). These three new films either did not fold, or only showed negligible folding, in response to each solvent. Altogether, these results further confirmed that the driving force behind the observed folding in the MIL-88A@PVDF films was the reversible expansion/contraction of MIL-88A crystals.

Next, we sought to investigate the self-folding properties of these MIL-88A@PVDF strips exposed to different levels of relative humidity. For this, we measured the folding angle (φ) (Supporting Information, Figure S18), from the original shape of each MIL-88A@PVDF strips (previously dried at 120 ºC) to the final shape resulting from each exposure (Figure 2a, and Supplementary Videos 1 and 2). Figure 2b shows the bending kinetics of strips subjected to relative humidity from 20% to 90%, for 30 min. At 20% relative humidity, no detectable changes were registered. However, from 40% to 90%, the folding response increased, with a similar $\varphi(t)$ profile in all cases. For example, at 70% relative humidity, the composite strip reached a maximum φ of ~ 105°, whereas at 90%, the maximum φ was 370°.

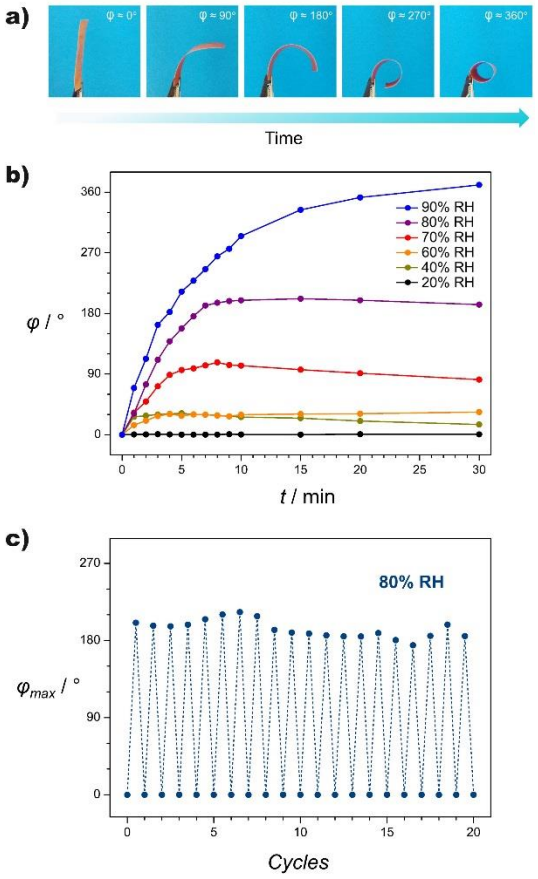

Figure 2 a) Photographs of MIL-88A@PVDF strips at different folding angles. b) Temporal change in the folding angle of a MIL-88A@PVDF strip at different levels of relative humidity (RH). c) Change in the maximum folding angle of a MIL-88A@PVDF strip over 20 cycles upon activation at 120 ºC and subsequent exposure to 80% relative humidity.

The steady-state folding angle reached for the MIL-88A@PVDF strips with a 50% (wt%) MOF content exposed to different levels of relative humidity correlated well with the water sorption isotherm collected on a MIL-88A@PVDF film (Figure 3). This isotherm showed a water uptake of 6% (wt%) at a relative humidity of 20% (Figure 3a), which has been ascribed to the sorption of H_2O molecules on the external surface of MIL-88A crystals.[27] The water uptake remained nearly constant from 20% to 45% relative humidity, after which point it sharply increased, ultimately reaching 18% (wt%) at 90% relative humidity. Figure 3b shows a similar trend for the folding angle, which abruptly increased starting from 60% relative humidity. These two steep increases in slope coincide with the characteristic transition phase from the closed form to the open form of MIL-88A, as recorded using humidity-controlled XRPD measurements (Figure 3c). Indeed, while the characteristic XRPD pattern of the closed form was retained up to a relative humidity of 45%, the characteristic peaks of the open form became apparent at 65%.

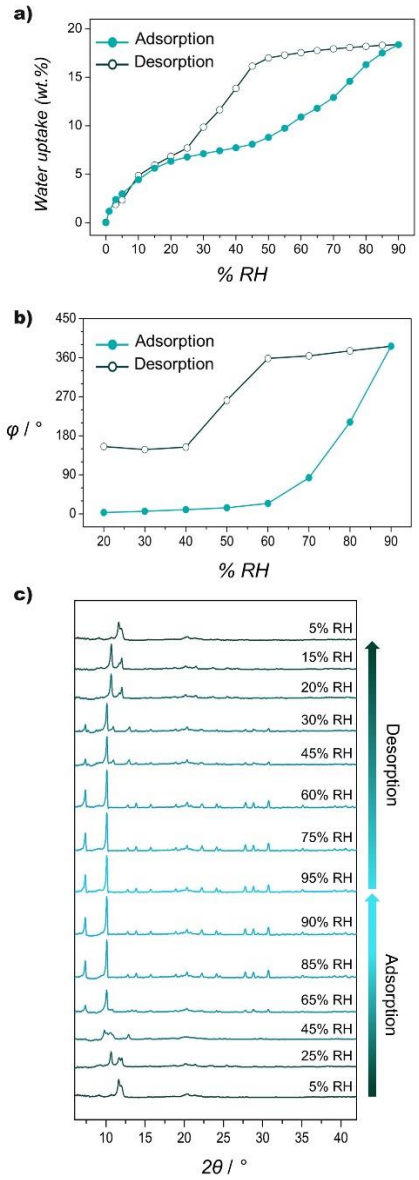

Figure 3 *a*) Water-vapour adsorption isotherm for a MIL88A@PVDF film at 25 ºC. Solid circles: adsorption; Empty circles: desorption. b) Change in folding-angle of a MIL88A@PVDF strip under relative humidity (RH) progressively increasing from 20% to 90% (solid circles), and then decreasing back to 20% (empty circles). c) *In situ* XRPD of a MIL88A@PVDF film undergoing water-vapour adsorption and desorption.

In the desorption branch, upon reducing the relative humidity from 60% back down to 20%, we observed a corresponding drop in slope that defined a large hysteresis loop. Analogously to the trend described above for sorption, this abrupt desorption of water molecules correlated well with humidity-controlled XRPD patterns of the reverse transition, from open form back to closed form (Figure 3c). Interestingly, the hysteresis observed on the water sorption/desorption cycle translated to the folding response of the MIL-88A@PVDF strips, thereby inducing a shape-memory effect from 90% down to 60% relative humidity (Figure 3b and Figure S19).

Based on the above trends, we reasoned that through rational choice of flexible MOF crystals having distinct adsorption/desorption profiles, we could selectively design soft materials that would exhibit predictable behaviour. Importantly, the self-folding capacity of a

MIL-88A@PVDF strip was maintained for at least 20 cycles of sequential exposure to a relative humidity of 80% and activation at 120 ºC (Figure 2c and Figures S20-21). Additionally, a similar actuation could be induced by exposing the MIL-88A@PVDF strips to vapours of the same organic solvents (*e.g.* methanol, acetone and acetonitrile) that triggered the bending of the film in the liquid state (Supporting Information, Figure S22 and Supplementary Video 3).

Finally, as proof-of-concept of the functional utility of such soft materials, we explored the ability of MIL-88A@PVDF composite films to lift heavy cargo, and their utility for generating 3D objects from 2D patterns. Thus, a 3 x 1 cm MIL-88A@PVDF strip (43 mg) exposed to a relative humidity of 90% was able to lift a 100-mg piece of glass (Figure 4a); meaning that this composite strip can lift objects 230% its own weight. Next, a 2D pattern comprising four triangular filter papers attached with three MIL-88A@PVDF strips was subjected to a relative humidity of 90%, leading to assembly of a 3D tetrahedron (Figure 4b and Supplementary Video 4).

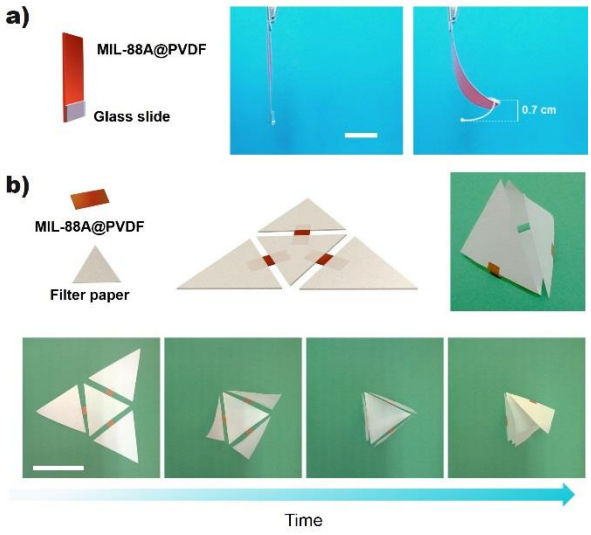

Figure 4 a) Photograph of a MIL-88A@PVDF strip lifting a 100-mg weight. Scale bar = 1 cm. b) Schematic representation (top), and temporal change in structure from a 2D pattern to a 3D tetrahedron (bottom), of composite strips subjected to 90% relative humidity. Scale bar = 5 cm.

In conclusion, we have demonstrated that self-folding soft materials can be built by incorporating flexible MOF crystals (as fillers) into polymer matrices. As a representative example, we added flexible MIL-88A crystals to a PVDF polymer matrix to synthesise a MIL-88A@PVDF composite film whose self-folding properties depend on the solvent and the relative humidity and correlate directly with the swelling properties of the MIL-88A crystals. Our strategy should enable the selective design and fabrication of new autonomous soft materials, whose properties could be tailored through strategic choice of the many available flexible MOFs with diverse adsorption-desorption profiles.

Acknowledgements

This work was supported by the Spanish MINECO (project PN MAT2015-65354-C2-1-R); the Catalan AGAUR (project 2014 SGR 80); the ERC, under EU-FP7 (ERC-Co 615954); MINECO and Junta de Andalucía (projects MAT2013-41836-R and P12-FQM-1656). It was also funded by the CERCA Programme/Generalitat de Catalunya. ICN2

acknowledges the support of the Spanish MINECO through the Severo Ochoa Centres of Excellence Programme, under grant SEV-2013-0295.

References

[1] S. Horike, S. Shimomura, S. Kitagawa, *Nat. Chem.* **2009**, *1*, 695.

[2] a) A. Schneemann, V. Bon, I. Schwedler, I. Senkovska, S. Kaskel, R. A. Fischer, *Chem. Soc. Rev.* **2014**, *43*, 6062-6096; b) F.-X. Coudert, *Chem. Mater.* **2015**, *27*, 1905-1916; c) J.-P. Zhang, H.-L. Zhou, D.-D. Zhou, P.-Q. Liao, X.-M. Chen, *Natl. Sci. Rev.* **2017**; d) S. Bureekaew, S. Shimomura, S. Kitagawa, *Sci. Technol. Adv. Mater.* **2008**, *9*, 014108; e) K. Uemura, R. Matsuda, S. Kitagawa, *J. Solid State Chem.* **2005**, *178*, 2420-2429; f) A. J. Fletcher, K. M. Thomas, M. J. Rosseinsky, *J. Solid State Chem.* **2005**, *178*, 2491-2510.

[3] a) N. Lock, Y. Wu, M. Christensen, L. J. Cameron, V. K. Peterson, A. J. Bridgeman, C. J. Kepert, B. B. Iversen, *J. Phys. Chem. C* **2010**, *114*, 16181-16186; b) Y. Wu, A. Kobayashi, G. J. Halder, V. K. Peterson, K. W. Chapman, N. Lock, P. D. Southon, C. J. Kepert, *Angew. Chem.* **2008**, *120*, 9061-9064.

[4] a) J. Seo, R. Matsuda, H. Sakamoto, C. Bonneau, S. Kitagawa, *J. Am. Chem. Soc.* **2009**, *131*, 12792-12800; b) D. Fairen-Jimenez, S. A. Moggach, M. T. Wharmby, P. A. Wright, S. Parsons, T. Düren, *J. Am. Chem. Soc.* **2011**, *133*, 8900-8902.

[5] a) S. Yang, X. Lin, W. Lewis, M. Suyetin, E. Bichoutskaia, J. E. Parker, C. C. Tang, D. R. Allan, P. J. Rizkallah, P. Hubberstey, N. R. Champness, K. Mark Thomas, A. J. Blake, M. Schröder, *Nat. Mater.* **2012**, *11*, 710; b) T. K. Maji, R. Matsuda, S. Kitagawa, *Nat. Mater.* **2007**, *6*, 142.

[6] a) G. Ferey, C. Serre, *Chem. Soc. Rev.* **2009**, *38*, 1380-1399; b) C. R. Murdock, B. C. Hughes, Z. Lu, D. M. Jenkins, *Coord. Chem. Rev.* **2014**, *258-259*, 119-136.

[7] a) C. Serre, F. Millange, S. Surblé, G. Férey, *Angew. Chem. Int. Ed.* **2004**, *43*, 6285-6289; b) C. Mellot-Draznieks, C. Serre, S. Surblé, N. Audebrand, G. Férey, *J. Am. Chem. Soc.* **2005**, *127*, 16273-16278; c) S. Surble, C. Serre, C. Mellot-Draznieks, F. Millange, G. Ferey, *ChemComm* **2006**, 284-286; d) C. Serre, C. Mellot-Draznieks, S. Surblé, N. Audebrand, Y. Filinchuk, G. Férey, *Science* **2007**, *315*, 1828-1831.

[8] a) P. Horcajada, F. Salles, S. Wuttke, T. Devic, D. Heurtaux, G. Maurin, A. Vimont, M. Daturi, O. David, E. Magnier, N. Stock, Y. Filinchuk, D. Popov, C. Riekel, G. Férey, C. Serre, *J. Am. Chem. Soc.* **2011**, *133*, 17839-17847; b) M. Ma, A. Bétard, I. Weber, N. S. Al-Hokbany, R. A. Fischer, N. Metzler-Nolte, *Cryst. Growth Des.* **2013**, *13*, 2286-2291.

[9] a) G. M. Whitesides, *Angew. Chem. Int. Ed.* **2018**, *57*, 1433-7851; b) F. Ilievski, A. D. Mazzeo, R. F. Shepherd, X. Chen, G. M. Whitesides, *Angew. Chem. Int. Ed.* **2011**, *50*, 1890-1895.

[10] a) Z. Liu, P. Calvert, *Adv. Mater.* **2000**, *12*, 288-291; b) S. M. Mirvakili, I. W. Hunter, *Adv. Mater.* **2018**, *30*, 1704407.

[11] a) R. Liu, X. Kuang, J. Deng, Y. C. Wang, A. C. Wang, W. Ding, Y. C. Lai, J. Chen, P. Wang, Z. Lin, H. J. Qi, B. Sun, Z. L. Wang, *Adv. Mater.* **2018**, *30*, 1705195; b) M. Ma, L. Guo, D. G. Anderson, R. Langer, *Science* **2013**, *339*, 186-189.

[12] a) J. Guan, H. He, L. J. Lee, D. J. Hansford, *Small* **2007**, *3*, 412-418; b) T. S. Shim, S. H. Kim, C. J. Heo, H. C. Jeon, S. M. Yang, *Angew. Chem. Int. Ed.* **2012**, *51*, 1420-1423; c) R. F. Donnelly, T. R. R. Singh, M. J. Garland, K. Migalska, R. Majithiya, C. M. McCrudden, P. L. Kole, T. M. T. Mahmood, H. O. McCarthy, A. D. Woolfson, *Adv. Funct. Mater.* **2012**, *22*, 4879-4890.

[13] Y. Liu, K. He, G. Chen, W. R. Leow, X. Chen, *Chem. Rev.* **2017**, *117*, 12893-12941.

[14] L. Suyi, K. W. Wang, *Bioinspiration Biomim.* **2017**, *12*, 011001.

[15] a) G. Stoychev, S. Zakharchenko, S. Turcaud, J. W. C. Dunlop, L. Ionov, *ACS Nano* **2012**, *6*, 3925-3934; b) G. Stoychev, S. Turcaud, J. W. C. Dunlop, L. Ionov, *Adv. Funct. Mater.* **2013**, *23*, 2295-2300.

[16] R. Kempaiah, Z. Nie, *J. Mater. Chem. B* **2014**, *2*, 2357-2368.

[17] A. Rath, S. Mathesan, P. Ghosh, *Soft Matter* **2016**, *12*, 9210-9222.

[18] H. Arazoe, D. Miyajima, K. Akaike, F. Araoka, E. Sato, T. Hikima, M. Kawamoto, T. Aida, *Nat. Mater.* **2016**, *15*, 1084.

[19] J. Mu, C. Hou, H. Wang, Y. Li, Q. Zhang, M. Zhu, *Sci. Adv.* **2015**, *1* ,1500533.

[20] J. Kim, J. A. Hanna, M. Byun, C. D. Santangelo, R. C. Hayward, *Science* **2012**, *335*, 1201-1205.

[21] H. Deng, Y. Dong, C. Zhang, Y. Xie, C. Zhang, J. Lin, *Mater. Horizons* **2018**, *5*, 99-107.

[22] a) Z. L. Wu, M. Moshe, J. Greener, H. Therien-Aubin, Z. Nie, E. Sharon, E. Kumacheva, *Nat. Commun.* **2013**, *4*, 1586; b) Z. Wei, Z. Jia, J. Athas, C. Wang, S. R. Raghavan, T. Li, Z. Nie, *Soft Matter* **2014**, *10*, 8157-8162; c) H. Thérien-Aubin, Z. L. Wu, Z. Nie, E. Kumacheva, *J. Am. Chem. Soc.* **2013**, *135*, 4834-4839; d) R. M. Erb, J. S. Sander, R. Grisch, A. R. Studart, *Nat. Commun.* **2013**, *4*, 1712.

[23] H. Deng, Y. Dong, J.-W. Su, C. Zhang, Y. Xie, C. Zhang, M. R. Maschmann, Y. Lin, J. Lin, *ACS Appl. Mater. Interfaces.* **2017**, *9*, 30900-30908.

[24] J. Dechnik, J. Gascon, C. J. Doonan, C. Janiak, C. J. Sumby, Angew. Chem. Int. Ed. 2017, 56, 9292.

[25] B. Seoane, S. Sorribas, Á. Mayoral, C. Téllez, J. Coronas, *Microporous Mesoporous Mater.* **2015**, *203*, 17-23.

[26] a) M. S. Denny, S. M. Cohen, *Angew. Chem. Int. Ed.* **2004**, *54*, 9029-9032; b) J. B. DeCoste, J. M. S. Denny, G. W. Peterson, J. J. Mahle, S. M. Cohen, *Chem. Sci.* **2016**, *7*, 2711-2716. c) J. Troyano, O. Castillo, J. I. Martínez, V. Fernández-Moreira, Y. Ballesteros, D. Maspoch, F. Zamora, S. Delgado, *Adv. Funct. Mater.* **2018**, *28*, 1704040.

[27] M. Li, I. Katsouras, C. Piliego, G. Glasser, I. Lieberwirth, P. W. M. Blom, D. M. de Leeuw, *J. Mater. Chem. C* **2013**, *1*, 7695-7702.

[27] S. Radosta, *Mol. Nutr. Food Res.* **1985**, *29*, 92-92.